The Cryosphere Discuss., 6, 2005–2036, 2012
www.the-cryosphere-discuss.net/6/2005/2012/
doi:10.5194/tcd-6-2005-2012

The Cryosphere Discussions

Recession, thinning, and slowdown of Greenland's Mittivakkat Gletscher

S. H. Mernild[1], **N. T. Knudsen**[2], **J. C. Yde**[3], **M. J. Hoffman**[4], **W. H. Lipscomb**[4], **R. S. Fausto**[5], **E. Hanna**[6], **and J. K. Malmros**[7]

[1]Climate, Ocean, and Sea Ice Modeling Group, Computational Physics and Methods, Los Alamos National Laboratory, New Mexico, USA
[2]Department of Geoscience, Aarhus University, Aarhus, Denmark
[3]Sogn og Fjordane University College, Sogndal, Norway
[4]Climate, Ocean, and Sea Ice Modeling Group, Fluid Dynamics and Solid Mechanics, Los Alamos National Laboratory, New Mexico, USA
[5]Geological Survey of Denmark and Greenland, Denmark
[6]Department of Geography, University of Sheffield, UK
[7]Department of Geography and Geology, University of Copenhagen, Denmark

Received: 5 April 2012 – Accepted: 7 May 2012 – Published: 1 June 2012

Correspondence to: S. H. Mernild (mernild@lanl.gov)

Published by Copernicus Publications on behalf of the European Geosciences Union.

Abstract

Glaciers in Southeast Greenland have thinned and receded during the past several decades. Here, we document changes for the Mittivakkat Gletscher, the only glacier in Greenland with long-term mass balance observations and surface velocity measurements (since 1995). Between 1986 and 2011, this glacier shrank by 18 % in surface area, 20 % in mean ice thickness, and 33 % in volume. We attribute these changes to summertime warming and to drier winter conditions. Meanwhile, the annual mean ice surface velocity decreased by 30 %, likely as a dynamic result of thinning. This dynamic thinning is predicted by ice deformation theory but has rarely been observed on decadal time scales. Mittivakkat Gletscher summer surface velocities were on average 50–60 % above winter background values, and up to 160 % higher during peak velocity events. The transition from winter to summer values followed the onset of positive temperatures. Satellite observations show area losses for most other glaciers in the region; these glaciers are likely also to have lost volume (in average around one-third) and slowed down in recent decades.

1 Introduction

In recent decades, glaciers have thinned and receded in many regions of the world (Oerlemans et al., 2007; Cogley, 2012). The contribution of glacier mass loss to sea-level rise is comparable to that from the Greenland and Antarctic ice sheets and has increased in recent decades (Kaser et al., 2006; Meier et al., 2007; Cogley, 2012).

Thousands of individual glaciers are located peripheral to the Greenland Ice Sheet (GrIS), covering an area of $54\,400 \pm 4400\,\mathrm{km}^2$ (Radić and Hock, 2010), compared with $\sim 1.7 \times 10^6\,\mathrm{km}^2$ for the whole ice sheet (Kargel et al., 2011). The estimated volume of these glaciers is $17\,865 \pm 2993\,\mathrm{km}^3$, or a sea level equivalent (SLE) of 44 ± 7 mm. Among Earth's major glaciated regions (excluding the two large ice sheets) Greenland ranks fourth in glacier ice mass after Arctic Canada, Antarctica, and Alaska (Radić and

Hock, 2010). Our knowledge of the distribution and climate sensitivity of these glaciers is limited. Glacier mass-balance studies often exclude the Greenland peripheral glacier contribution to sea-level rise (e.g., Jacob et al., 2012), even though studies by Yde and Knudsen (2007), Kargel et al. (2011), and Mernild et al. (2012a) have documented substantial glacier area recession on Disko Island (69–70° N; West Greenland), in Central East Greenland (68° N–72° N), and in the Ammassalik region (65° N; Southeast Greenland), respectively. Not only is the glacier area decreasing, but also the annual surface melt extent and the amount of surface melting and freshwater runoff have increased during the past several decades, both from peripheral glaciers and from the GrIS (e.g., Mernild and Hasholt, 2006; Hanna et al., 2008; Mernild et al., 2010; Mernild and Liston, 2012), influencing glacier dynamics through changes in subglacial hydrology (e.g., van der Wal et al., 2008; Sundal et al., 2011).

Mittivakkat Gletscher (henceforth MG; Fig. 1), located in the Ammassalik region, is Greenland's only peripheral glacier for which there exist long-term surface mass balance (SMB) records and surface velocity measurements (since 1995), and satellite margin and area observations (since 1986). This study focuses on changes in MG's SMB (winter, summer, and annual net mass balances), area cover, thickness, volume, and surface velocity during a 25-yr period of climate warming (1986–2011). Based on measurements we estimate trends in winter, summer, and net mass balances and quantify the decreases in MG area, mean ice thickness, and volume. We also analyze the subsequent impacts on glacier dynamics based on observed seasonal and mean annual ice surface velocity. We suggest that climate warming and reduced winter precipitation in the Ammassalik region have caused the MG to thin and retreat, with a resulting decrease in surface velocity. Based on area losses by other glaciers in the Ammassalik region, we suggest that the changes in MG are not merely a local phenomenon but are typical of the region.

2 Study area

The Mittivakkat Gletscher (65°41 N, 37°48 W; 26.2 km^2) is located in the Ammassalik region, Southeast Greenland (Fig. 1a). Long-term observations of both glacier front fluctuations (since the maximum Little Ice Age (LIA) extension around 1900) and SMB (since 1995) exist. Since the LIA the MG has undergone almost continuous retreat (Knudsen and Hasholt, 1999; Knudsen et al., 2008; Mernild et al., 2011a). During 1986–2011 the glacier area decreased by 18 %, from 31.6 km^2 to 26.2 km^2 (Fig. 1b), and the mean surface slope increased from 0.095 to 0.104 m m^{-1}. The area retreat follows the overall trend for the Ammassalik region, where glacier area fell by 27 ± 24 % during this period (Mernild et al., 2012a). (Here and below, the error term is the standard deviation among 35 glaciers.) The MG is a temperate valley glacier with mean annual isothermal conditions near 0 °C, apart from the upper few meters that undergo seasonal temperature variations (Knudsen and Hasholt, 1999). Since 1995 the equilibrium line altitude (ELA; the spatially averaged elevation of the equilibrium line, defined as the set of points on the glacier surface where the net mass balance is zero) has risen from around 500 m above sea level (a.s.l.) to 750 m a.s.l. The average accumulation-area ratio (AAR, the ratio of the accumulation area to the area of the entire glacier) is about 0.10 (updated from Mernild et al., 2011a), indicating that MG is significantly out of balance with the present climate. The glacier will likely lose at least 70 % of its current area and 80 % of its current volume even in the absence of further climate warming (Mernild et al., 2011a).

3 Data and methods

3.1 Area, thickness, and volume

The MG and its surrounding landscape have been observed by Landsat satellite imagery since 1972. Here we use data from the Landsat 5 Thematic Mapper (TM) and

Landsat 7 Enhanced Thematic Mapper 10 Plus (ETM+), each having a ground resolution of 30 m (15 m in the panchromatic band), and from the Advanced Spaceborne Thermal and Reflection Radiometer (ASTER) Global Digital Elevation Model Version 2 (GDEM v2), with a ground resolution of 30 m. These data were used to map the MG margin position, area, and marginal recession for 1986, 1999, and 2011. Satellite images were obtained from cloud-free scenes (<25 % cloud cover) at the end of the melt season (September 1986, September 1999, and August 2011). Horizontal errors associated with the different scenes and sensors were ±15 m (TM), ±15 m (7.5 m panchromatic) (ETM+), and ±15 m (ASTER GDEM v2). The vertical error associated with the ASTER GDEM v2 is approximately ±12.5 m across the Greenland region (Tachikawa et al., 2011). Detailed satellite image specifications are shown in Mernild et al. (2012a).

In 1994 the MG surface elevation, bed topography, and ice thickness were estimated based on monopulse radio-echo soundings (Knudsen and Hasholt, 1999). The mean MG ice thickness (115 m) was derived from measurements at 450 positions, spaced about 100 m apart along profiles running across the MG, and about 300 m apart along the flow with a vertical spacing of 50 m. The error of the measured ice thicknesses was estimated to be less than ±5 m (Knudsen and Hasholt, 1999), giving a relative uncertainty of less than 5 % for the mean ice thickness.

In 1995 a glacier observation program was initiated to measure MG's annual SMB and to map changes in ice thickness. The SMB has been measured annually each year (September through August). In 10 out of 16 yr (Fig. 2), both winter balances (accumulation in September through May) and summer balances (ablation in June through August) were observed. A network of stakes was used to measure net summer ablation (Fig. 1a) based on the direct glaciological method (Østrem and Brugman, 1991). Cross-glacier stake lines were deployed at separations of approximately 500 m, with stakes 200–250 m apart in each line. Measurements were obtained at 59 stakes covering 16.3 km^2 of the MG, excluding the crevassed area in the southeastern part of the glacier (this omission is not likely to bias the results). Since its establishment the stake network has moved slowly down the glacier by 50–275 m. (This movement has

Discussion Paper | Discussion Paper | Discussion Paper | Discussion Paper |
TCD
6, 2005–2036, 2012
Recession of Greenland's Mittivakkat Gletscher
S. H. Mernild et al.

an insignificant impact on estimates of the mean annual surface velocity.) The end-of-winter snow density was measured vertically at 25 cm depth intervals in snow pits at 250, 500, and 750 m a.s.l., and was used for calculations of the snow water equivalent. The winter balance was calculated as the difference between the net annual balance and the summer balance. The mass balance observations are thought to be accurate within 15 % for the MG (Knudsen and Hasholt, 2004), which is within the uncertainty range suggested by Cogley and Adams (1998).

The observed MG ice volume was estimated for 1986, 1999, and 2011 (the same years as the area extent derived from Landsat imagery) based on the satellite-derived glacier extent multiplied by the mean ice thickness. The mean ice thickness for 1999 and 2011 was calculated from the observed 1994 mean thickness minus the cumulative observed net ablation (Fig. 2). The 1986 mean ice thickness was estimated by adding to the 1994 mean thickness the net ablation during 1986–1994, based on a linear extrapolation of the observed 1995/96 to 2010/11 net mass balance. This is a simple approximation of the 1986 mean ice thickness, but we have confidence in the method, since the trends in air temperature and precipitation for the region during 1995–2011 are consistent with trends for 1986–1995 (Mernild et al., 2012b).

3.2 Surface ice velocity and thickness changes

Each stake position (Fig. 1) was measured annually. Before 2004, the positions were measured by topographic surveys using a theodolite (Kern) with an Electro-optical Distance Meter, having a horizontal uncertainty of less than ±1 m. After 2004, position was based on a portable single-frequency GPS (Garmin GPS 12 XL) with a relative uncertainty of about ±2 m; this value is based on repeated fixed station measurements with the same instrument during several years. The annual stake positions were used to calculate the spatial mean surface velocity field for the MG. Also, a continuous ice surface velocity time series was obtained from a dual-frequency GPS-receiver (Javad Laxon GGD160T, operated by the Geological Survey of Denmark and Greenland) near the center of the MG (Fig. 1a). This time series was used to determine the seasonal variability in ice surface velocity. However, we have access to data only from May 2004 through July 2005 (when the receiver was located at elevations from 462 to 455 m a.s.l.) and from March 2009 through August 2010 (513 to 509 m a.s.l.). The horizontal and vertical uncertainty in the GPS time series were on average around 3 mm and 6 mm, respectively.

Thickness changes, $\mathrm{d}h/\mathrm{d}t$, at a point on the glacier are a combination of SMB and vertical strain, and they can be described by continuity (Cuffey and Patterson, 2010) approximately as:

$$\mathrm{d}h/\mathrm{d}t = b - u_\mathrm{s} \tan\alpha + w_\mathrm{s} \tag{1}$$

where b is the SMB, u_s is the horizontal surface velocity, α is the surface slope, and w_s is the vertical velocity of a fixed point on the glacier (e.g., the top of a stake). However, our surveys measured the position of the ice surface at each stake, and therefore our observed vertical velocity includes the SMB, b. Thus, we calculate thickness changes as:

$$\mathrm{d}h/\mathrm{d}t = w_\mathrm{obs} - u_\mathrm{s} \tan\alpha \tag{2}$$

where w_obs is the observed vertical velocity measured as the height difference between two successive surveys of the ice surface elevation at the position of a stake. We separate the component of thickness change due to vertical strain rate (emergence velocity) as:

$$w_\mathrm{e} = \mathrm{d}h/\mathrm{d}t - b \tag{3}$$

3.3 Meteorological data and river discharge

Meteorological conditions at MG were obtained from automated weather stations located on a small nunatak (515 m a.s.l.; operated by University of Copenhagen) (Mernild et al., 2008) a few hundred meters below the present ELA, and in the outskirts of

Tasiilaq (44 m a.s.l.; operated by Danish Meteorological Institute) (DMI 2011), located 15 km to the southeast of MG. Also, seasonal variations in observed river discharge draining directly from MG were obtained from June–August 2004, August 2009, and July–August 2010 (Hasholt and Mernild, 2006; Mernild and Hasholt, 2006; Liston and Mernild, 2012). River discharge was measured 1.5 km downstream from the MG front in the proglacial valley above Sermilik Fjord. Both observed river discharge and meteorological data (air temperature and precipitation) were compared to seasonal and annual changes in the MG ice surface velocity.

4 Results and discussion

4.1 Spatial surface mass balances

For MG the annual SMB has been observed for 16 years since 1995/96 and the winter and summer balances for 10 yr. During winter (September through May) the MG gains mass, and during summer (June through August) the MG loses mass. Both gains and losses are unevenly distributed in space and time. The mean annual net mass balance is -0.97 ± 0.19 m water equivalent (w.e.) yr^{-1}, with a mean winter balance of 1.18 ± 0.19 m w.e. yr^{-1} and a mean summer balance of -1.94 ± 0.38 m w.e. yr^{-1} (Figs. 2 and 3). The net annual SMB has decreased on average by 0.09 m w.e. yr^{-2} ($r^2 = 0.36$; $p < 0.01$, significant, where r^2 is the explained variance and $p$is level of significance). The computed trends in the winter and summer balances are smaller, probably because these balances were not observed during several years in the later part of the record with highly negative annual SMB. The net balance in 2010/11 was a record-setting −2.45 m w.e., about 2 standard deviations below the mean and 0.29 m w.e. more negative than the previous observed record low mass balance in 2009/10 (Mernild et al., 2011b).

Figure 3 illustrates the spatial variation in winter, summer, and annual net mass balances. The mean winter balance shows less accumulation at low elevations

(0.3 m w.e. yr^{-1}) than at higher elevations (above 1.4 m w.e. yr^{-1}) (Fig. 3a), with a mean orographic gradient of about 0.2 m w.e. yr^{-1} per 100 m increase in elevation. Since 1995/96 the mean annual accumulation has decreased (Fig. 2). Figure 3a illustrates the spatial distribution of the annual change in winter balance, showing that the terminus, the marginal areas at high elevations, and areas near mountain ridges had the smallest decrease, and in some areas an increasing winter balance (0.04 m w.e. yr^{-2}). The largest decreases (−0.20 m w.e. yr^{-2}) occurred at the center line of the glacier and at higher elevations, most pronounced at about 500 m a.s.l. Meteorological observations at MG show that the mean annual wind speed has increased in recent years (Mernild et al., 2008). Also, katabatic winds from the north and east (dominating around 50 % of the time) were stronger at the center of the MG than near the margins. The inhomogeneous annual change in winter accumulation can therefore likely be linked to increasing wind speed and snow redistribution. Snow usually begins to drift at a wind speed above 5.0 m s^{-1} (Liston and Sturm, 1998). For MG the mean winter speed for snow drifting was exceeded 29 % of the time, with a slightly increase in recent years (Mernild et al., 2008).

The summer balance shows more ablation at low elevations and decreasing mass loss towards higher elevations (Fig. 3b), as expected. The summer mass balance varied from −3.6 m w.e. yr^{-1} at low elevations to −1.4 m w.e. yr^{-1} at high elevations, giving a mean gradient of 0.3 m w.e. yr^{-1} per 100 m increase in elevation. Figure 3b illustrates the spatial distribution of the annual change in summer balance, showing the largest change towards the margins, most pronounced in the southern part of the glacier (−0.22 m w.e. yr^{-2}). A possible explanation for this pattern is that as the margins receded, the reflection of radiation and convection of heat from the surrounding areas increased, causing more melting, whereas towards the center of the glacier the energy balance was less affected (Fig. 3b).

The net mass balance shows the combined effects of changes in winter and summer balances. The net mass balance shows the greatest net ablation at low elevations (−3.0 m w.e. yr^{-1}) and lowest values at higher elevations (0.4 m w.e. yr^{-1}), with the

ELA located around 750 m a.s.l. (Fig. 3c). The mean net mass balance gradient was 0.5 m w.e. yr^{-1} per 100 m. The annual change in net mass balance is inhomogeneous, with the largest changes in the marginal area to the south (-0.24 m w.e. yr^{-2}) and at the center line (around -0.16 m w.e. yr^{-2}). The increasing mass loss at ∼500 m a.s.l. probably reflects that in this area, more ice has been exposed in recent years compared to previous periods when mainly snow and firn were exposed at the surface.

4.2 Area and volume changes

The glacier-covered area is one of the easiest glacier morphometric quantities to measure (Bahr, 2011). For MG the surface area was estimated for the years 1986, 1999, and 2011 based on satellite imagery. The area decreased by 18 % during this period, from 31.6 km^2 (1986) to 29.5 km^2 (1999) to 26.2 km^2 (2011) (Fig. 4; updated from Mernild et al., 2012a). For the same period, the estimated mean ice thickness fell by 20 %, from 122 m (1986) to 111 m (1999) to 98 m (2011). Based on observed changes in area cover and mean thickness, the mean volume fell by 1.33 km^3 (33 %) (Fig. 4), from 3.90 km^3 (1986) to 3.36 km^3 (1999) to 2.57 km^3 (2011). Knudsen and Hasholt (2004) estimated a volume loss of 0.0116 km^3 yr^{-1} during 1995–2002 based on changes in mean ice thickness from SMB observations. If this trend is extrapolated over a fixed area of 31.6 km^2 for the 25-year period (1986–2011), the total volume loss would be only 0.53 km^3. If the 1995–2011 SMB observations are used for the 25-yr period, the volume loss would be 0.77 km^3 (only around 60 % of the estimated 1.33 km^3 volume loss). This shows that if area changes are not included, volume changes will be underestimated.

The volume decrease was simultaneous with an observed increase in mean annual air temperature (MAAT) and a decrease in mean annual precipitation (uncorrected) of 0.09 °C yr^{-1} and -5 mm w.e. yr^{-2} (1995–2011), respectively, at the DMI Station in Tasiilaq. Climate records from other meteorological stations in Southeast Greenland show significant warming since the early 1980s (e.g., Mernild et al., 2011a), suggesting that the MG recession is likely not merely a local phenomenon, but indicative of glacier changes in the broader region. Indeed, the MG area loss is consistent with satellite-derived surface area changes from 35 glaciers in the Ammassalik region, illustrating area losses of 27 ± 24 % during 1986–2011 (Mernild et al., 2012a).

The current decrease in glacier volume is an important component of global sea-level rise (Kaser et al., 2006; Meier et al., 2007; Cogley, 2012). MG is the only glacier in Greenland for which volume changes can be estimated from direct observations. Globally, volume has been measured directly for fewer than 200 glaciers, since observations require considerable time and expense (Bahr, 2011). Glacier volume (V), however, can be estimated from the surface area (A) using a power-law scaling relationship (Bahr et al., 1997):

$$V = cA^{\gamma} \tag{4}$$

where γ and c are derived from data and theory, and typical values are $\gamma = 1.36$ and $c = 0.033\,\mathrm{km}^{3-2\gamma}$ for valley glaciers (Chen and Ohmura, 1990; Bahr, 1997; Bahr et al., 1997). For the MG, the mean volume values implied by the scaling function for 1986, 1999, and 2011 are 3.66 km^3, 3.43 km^3, and 2.80 km^3, respectively, close to the observation-based estimates of 3.90 km^3, 3.35 km^3, and 2.55 km^3. The volume loss calculated from the scaling function (Eq. 4) is 25 %, close to the 33 % estimated from observations.

The good agreement between these two estimates suggests that area-volume scaling could appropriately be applied to other glaciers in the Ammassalik region. Based on the satellite-derived surface areas for 1986, 1999, and 2011 from the 35 observed glaciers (Fig. 7 in Mernild et al., 2012a), the mean volume loss over 25 yr was 33±28 %, varying from a maximum loss of 85 % to a maximum gain of 46 %. Three glaciers out of 35 gained mass, all around 1 km^2 in area and facing west. This analysis suggests that GIC in the Ammassalik region on average lost about one-third of their volume since 1986. If the warming of recent decades is not reversed, glacier retreat will likely continue, and many glaciers in the region will shrink dramatically. To confirm this suggested trend, more volume estimates from glaciers peripheral to the GrIS would be needed.

4.3 Surface velocity and thickness changes

The mean annual surface velocity of MG has been observed since 1995/96 at stake locations (Fig. 1). The spatial distribution of the mean surface velocity has a maximum of 22 m yr^{-1} near the center line. The velocity decreases to ∼3–5 m yr^{-1} at the lateral margins (Fig. 5a) as a result of drag from the valley walls and low ice thickness (e.g., Cuffey and Paterson, 2010). The highest surface velocities are observed where the ice is thickest (Fig. 5b), consistent with theory suggesting that the surface velocity is proportional to H^{n+1}, where H is the ice thickness and n is usually taken as 3, when the motion is primarily driven by the shear stresses in the horizontal plane (Payne and Dongelmans, 1997). Over the 15-year period (1996/97–2010/11), surface velocity has fallen across the glacier, with decreases of over 50 % in much of the ablation zone. However, the change in mean annual surface velocity has been unevenly distributed across the glacier (Fig. 5a). The greatest decrease, about 0.6 m yr^{-2}, is observed on the lower part of the glacier near the margins (Fig. 5a), where the greatest mass loss has also occurred (Fig. 5c).

Surface elevation and thickness also decreased across the glacier from 1995–2011 (Fig. 5c). The longitudinal profile shows a surface elevation change due to SMB of −25 to −44 m w.e. (averaging −37 m w.e.) in the lower part of the glacier at stakes 31, 40, 50, 60, and 70, and −6 to −12 m w.e. (averaging −8 m w.e.) in the upper part at stakes 110, 120, 130, and 140 (Fig. 5d, red line). If both the SMB observations and the vertical velocity (w_e) calculations (Eqs. 1 to 3) are included in the surface elevation calculations for the longitudinal MG profile, the surface change would instead be −6 to −20 m w.e. (averaging −14 m w.e.) on the lower part of the MG, and −4 to −10 m w.e. (averaging −6 m w.e.) at the upper part (Fig. 5d, green line) (Fig. 5d, blue line). Overall, vertical strain was able to compensate for about 50 % of the elevation change due to the SMB alone. The vertical strain was unevenly distributed along the longitudinal profile

(Fig. 5d), with the greatest compensation at central elevations at stake 80 ($w_e = 20$ m) where the mean surface velocity was greatest, and decreasing towards high and low elevations.

The decrease in mean annual velocity observed across MG could be due to a decrease in ice deformation or a decrease in basal sliding (Fig. 5a). To assess the role of changes in deformation, we calculate the theoretical surface velocity due to deformation at the beginning and end of the study period using the shallow ice approximation (Hutter, 1983) as:

$$v_{sia} = 1/2A\left(\rho g \mathrm{d}S/\mathrm{d}x\right)^3 H^4 \quad (5)$$

where A is the flow law rate factor, taken as $2.1 \times 10^{-16}\,\mathrm{yr^{-1}\,Pa^{-3}}$ for isothermal ice at 0 °C (Cuffey and Paterson, 2010), ρ is the density of ice, taken as $900\,\mathrm{kg\,m^{-3}}$, g is acceleration due to gravity, $9.81\,\mathrm{m\,s^{-2}}$, $\mathrm{d}S/\mathrm{d}x$ is the surface slope, and H is the ice thickness. We apply Eq. (1) at stake 60 in the center of the ablation zone where the shallow ice approximation is likely to be valid for the beginning and end of the study period (Table 1). At this representative location, the change in calculated deformation rate over the study period ($12\,\mathrm{m\,yr^{-1}}$) accounts for the change in observed surface velocity ($11\,\mathrm{m\,yr^{-1}}$). The decrease in glacier slope at stake 60 (Table 1) accounts for less than 10 % of the calculated change in deformation, with the remainder due to the change in thickness. Although the calculated velocity is approximate, we consider this strong evidence that the thinning of the glacier is the primary cause of the observed slowdown. Furthermore, mean annual surface velocity averaged over the entire glacier is positively correlated with glacier-averaged ice thickness over the study period ($r^2 = 0.77$, significant at $p < 0.01$, Fig. 6).

The alternative hypothesis is that a reduction in basal sliding has resulted in the observed surface velocity decrease of over 50 %. Such a reduction in sliding would have to have occurred despite an increasing trend in meltwater production (and an increasing negative summer balance, Fig. 3) over most of MG during the study period. The effects of meltwater production on basal sliding are complex. There is evidence that increased penetration of surface meltwater to the ice-bedrock interface can accelerate the flow (Zwally et al., 2002; Parizek and Alley, 2004), but it has been shown that increased summer melt does not necessarily lead to increased velocities for mountain glaciers (Truffer et al., 2005; Vincent et al., 2009) and for sectors of the GrIS (van der Wal et al., 2008; Sundal et al., 2011). Instead, englacial and subglacial drainage systems can continually adjust to variable meltwater production (Bartholomaus et al., 2008; van der Wal et al., 2008; Bartholomew et al., 2010; Schoof, 2010; Hoffman et al., 2011; Sole et al., 2011; Sundal et al., 2011), minimizing changes in basal sliding rates and potentially resulting in less sliding at higher melt rates than low melt rates (Sundal et al., 2011).

Alhough calculating the dynamic effect of changes in meltwater production is beyond the scope of this paper, we do see evidence that changes in melt have only a minor impact on surface velocity. Summer mass balance and mean June-July-August (JJA) temperatures, both proxies for melt, have weak negative correlation with mean annual surface velocity ($r^2 = 0.23$, significant at $p < 0.05$, and $r^2 = 0.30$, significant at $p < 0.025$, respectively, Fig. 6). Thus higher melt appears to correlate with higher velocities at MG, suggesting that increasing mean summer melt cannot explain the decreasing mean annual velocity.

Also, we can assess the decrease in sliding that would be required to explain the observed slowdown if deformation had remained constant. Daily surface velocity was observed during two periods in the latter part of the study period (May 2004 through July 2005, and March 2009 through August 2010) (Fig. 7a) near the center of MG (see Fig. 1 for locations of the GPS stations). The mean annual surface velocity of 22 m yr^{-1} is composed of two periods: a winter period lasting about 9 months with an average velocity of ∼0.04 m d^{-1} and a summer period lasting about 3 months with an average velocity of ∼0.06 m d^{-1}. If we assume that sliding is negligible during winter, we can estimate that there is about 0.04 m d^{-1} of deformation at this location and therefore about 0.02 m d^{-1} of sliding during summer. If deformation had not changed during the study period, the summer sliding rate would need to be 0.08 m d^{-1} (or four times higher than current) at the start of the study period to obtain the observed surface velocity of

TCD
6, 2005–2036, 2012

22 m yr^{-1} at the start of the study. Such a change seems unrealistic and is at odds with the negative correlation between summer mass balance and surface velocity shown in Fig. 6.

Based on these analyses, there is strong evidence that the observed decadal slowdown is due to decreasing deformation as the ice has thinned, and that changing hydrology is of secondary importance. Although such a relationship between thickness and velocity is expected from the theory of nonlinear plastic deformation of ice, it has rarely been observed at decadal timescales, presumably due to the rarity of long-term thickness and velocity records. Vincent et al. (2009) recorded 20 yr of thickening and speedup followed by 30 yr of thinning and slowdown at Glacier d'Argentière, France. Müller and Iken (1973) found small (∼1 m) thickness changes inadequate to explain annual velocity changes over 2–3 yr periods on White Glacier, Arctic Canada. Our observations provide a clear demonstration of slowdown associated with glacier thinning. Since other glaciers in the region are retreating and thinning, they are also likely to be slowing down, but this slowdown remains to be confirmed by observations.

On a seasonal scale, the daily MG surface velocity was observed during two periods (May 2004 through July 2005, and March 2009 through August 2010) (Fig. 7a) (see Fig. 1 for locations of the GPS stations). For the summer (June through August) the mean ice surface velocity varied between 0.061 and 0.066 m d^{-1}, with a maximum observed daily velocity of 0.10 m d^{-1}. For the winter (September through May) the velocity varied between 0.038 and 0.043 m d^{-1} during a period of little or no subglacial water. The summer values are 50–60 % higher than the winter background values, and up to 160 % higher for peak events (Fig. 7a and b). Surface velocity is significantly correlated with surface air temperature in summer but not in winter (Fig. 8). A similar seasonal pattern in ice surface velocity was observed at the John Evans Glacier, Nunavut, Canada (Bingham et al., 2003) and for the western land-terminating margin of the GrIS, where the peak summer velocity was up to 220 % above the winter background values (Bartholomew et al., 2010; Hoffman et al., 2011). MG peak velocity events were typically accompanied by uplift of a few centimeters. Similar uplift has been observed for the GrIS during ice motion speedup (e.g., Hoffman et al., 2011; Sole et al., 2011).

The seasonal pattern in the daily surface velocity seems visually to follow the observed surface air temperature and precipitation (rain) events. Following the onset of positive temperatures and rain events, the ice surface velocity increased above winter background values for up to 2–3 months, together with an observed increase in river discharge downstream (Fig. 7b). During and after high-temperature days, surface velocities increased rapidly (Fig. 7a and b), suggesting that meltwater production enhances ice motion when meltwater first reaches the ice-bed interface. Similar processes have been observed for the GrIS (e.g., Zwally et al., 2002; Shepherd et al., 2009; Bartholomew et al., 2010, 2011; Hoffman et al., 2011; Sole et al., 2011). However, the correlation between daily ice surface velocity and river discharge for MG is insignificant ($r^2 = 0.02$), suggesting that the amount of meltwater is not a dominant factor controlling basal ice velocities. The lack of a strong relationship is likely related to interactions of meltwater in subglacial channels with the distributed network of the subglacial drainage system, but changes in water storage may also be important (Bartholomaus et al., 2008; Schoof, 2010). The correlations between daily ice surface velocity and proglacial discharge in various summer months are also insignificant ($r^2 = 0.02$–0.04), indicating that seasonal variations in the subglacial drainage system have little or no influence on basal ice velocity.

During the summer a characteristic double peak in ice surface velocity was seen in all three observed years (Fig. 7a). The earlier peak occurs in the first half of the melt season (around June), and the later peak in the second half of the melt season (around August). The earlier peak appears to be driven by rising temperatures creating surface melt and subsequently increasing the englacial and subglacial storage (Bartholomaus et al., 2008) as meltwater drains into a hitherto inefficient distributed subglacial drainage system, raising the water pressure and enhancing basal ice motion. Bartholomew et al. (2010) found that a key control on the relationship between surface melting and surface ice velocity variations is the structure and the hydraulic efficiency of the subglacial drainage system, which evolves spatially and temporally during the melt season. After the initial velocity peak, the efficiency of the drainage system might increase due to continuous inflow of surface melt water, decreasing the water pressure and reducing the basal motion (e.g., Truffer et al., 2005; Schoof, 2010; Pimentel and Flowers, 2011). The velocity peak later in the melt season may be related to warmer air temperatures, at least for 2004 and 2010, causing a pulse of surface meltwater to enter the subglacial hydrology system and again increase the water pressure. Instead of a larger velocity speedup, however, a substantially smaller peak was observed because the subglacial hydrologic system has already evolved to handle meltwater inputs. High river discharge was observed at the same time as the velocity peak (Fig. 7b). For 2005, however, the late velocity peak seems to be initiated by a combination of increasing air temperature and rain events (Fig. 7a and b). The subsequent drop in ice surface velocity after the second peak might be due to a decrease in surface meltwater production during late summer.

5 Summary and conclusion

Direct mass balance observations from Greenland glaciers are rare, and the MG is the only such glacier with long-term mass balance observations. We have analyzed spatially distributed winter, summer, and annual mass balances and ice surface velocities based on direct observations of the MG, along with satellite-derived area cover. We have found unambiguous evidence of ice thinning, retreat, and slowdown in a warming climate. From 1986–2011 we found significant decreases in surface area (18 %), mean ice thickness (20 %), ice volume (33 %), and mean annual surface velocity (30 %). The decrease in surface velocity was likely a dynamic effect of ice thinning.

Since climate records from meteorological stations in Southeast Greenland suggest regional warming since the early 1980s, the MG recession is likely not a local phenomenon. Satellite-observed area losses for nearby glaciers, together with area-volume scaling relationships, suggest that ice volume for other glaciers in the region has declined by about one-third since 1986, similar to MG. It is likely that these glaciers also slowed down as a result of thinning. Observations of MG and nearby glaciers, as presented here, will be crucial for understanding the behavior of Greenland's peripheral glaciers in a warming climate.

Acknowledgements. This work was partly supported by the Climate Change Prediction Program and by the Scientific Discovery for Advanced Computing (SciDAC) program within the US Department of Energy's Office of Science and by a Los Alamos National Laboratory (LANL) Director's Fellowship. LANL is operated under the auspices of the National Nuclear Security Administration of the US Department of Energy under Contract No. DE-AC52-06NA25396), and partly from the European Community's Seventh Framework Programme under grant agreement No. 262693. Thanks are given to the Geological Survey of Denmark and Greenland (GEUS) for providing GPS-based surface velocity time series from the Mittivakkat Gletscher, to the University of Copenhagen for providing meteorological data from the Mittivakkat Gletscher (Station Nunatak) and proglacial observed river discharge, and to the Danish Meteorological Institute for providing WMO synoptic meteorological data from Tasiilaq. NTK, SHM, and JCY did the MG mass balance observations. SHM and NTK planned, analyzed the data, and wrote the manuscript, and JCY, MJH, WHL, EH, RSF, and JKM contributed to the discussion of results and writing of the text.

References

Bahr, D. B.: Global distribution of glaciers properties: a stochastic scaling paradigm, Water Resour. Res., 33, 1669–1679, 1997.

Bahr, D. B.: Estimation of glacier volume and volume change by scaling methods, 278–280, in: Encyclopedia of snow, ice, and glaciers, edited by: Singh, V. P., Singh, P., and Haritashya, U. K., Springer, Dordrecht, The Nederlands, 1253 pp., 2011.

Bahr, D. B., Meier, M. F., and Peckham, S.: The physical basis of glacier volume-area scaling, J. Geophys. Res., 102, 20355–20362, 1997.

Bartholomaus, T. C., Andersen, R. S., and Andresen, S. P.: Response of glacier basal motion to transient water storage, Nat. Geosci., 1, 33–37, doi:10.1038/ngeo.2007.52, 2008.

Bartholomew, I., Nienow, P., Mair, D., Hubbard, A., King, M., and Sole, A.: Seasonal evolution of subglacial drainage and acceleration in a Greenland outlet glacier, Nat. Geosci., 3, 408–411, 2010.

Bartholomew, I., Nienow, P., Sole, A., Mair, D., Cowton, T., Palmer, S., and Wadham, J.: Supraglacial forcing of subglacial drainage in the ablation zone of the Greenland ice sheet, Geophys. Res. Lett., 38, L08502, doi:10.1029/2011GL047063, 2011.

Bingham, R. G., Nienow, P., and Sharp, M. J.: Intra-annual and intra-seasonal flow dynamics of a High Arctic polythermal valley glacier, Ann. Glaciol., 37, 181–188, 2003.

Chen, J. and Ohmura, A.: Estimation of alpine glacier water resources and their change since the 1870s, International Association of Hydrological Sciences Publication, 193, 127–135, 1990.

Cogley, G.: The Future of the World's Glaciers. In The Future of the World's Climate, 197–222, doi:10.1016/B978-0-12386917-3.00008-7, 2012.

Cogley, J. G. and Adams, W. P.: Mass balance of glaciers other than the ice sheet, J. Glaciol., 44, 315–325, 1998.

Cuffey, K. M. and Paterson, W. S. B.: The Physics of Glaciers, Fourth edition, Elsevier, Oxford, UK, 707 pp., 2010.

DMI.: Weather and Climate Data from Greenland 1958–2010 – Descriptions and Documentation of Observations of Temperature, Precipitation, Wind, Cloud Cover, Air Pressure, Humidity and Depth of Snow, Technical Report, 11–10, available at: www.dmi.dk/dmi/tr11-10, 1–22, 2011.

Hanna, E., Huybrechts, P., Steffen, K., Cappelen, J., Huff, R., Shuman, C., Irvine-Fynn, T., Wise, S., and Griffiths, M.: Increased runoff from melt from the Greenland Ice Sheet: a response to global warming, J. Climate, 21, 331–341, doi:10.1175/2007JCLI1964.1, 2008.

Hasholt, B. and Mernild, S. H.: Glacial erosion and sediment transport in the Mittivakkat Glacier catchment, Ammassalik island, southeast Greenland, 2005, IAHS Publ. 306, 45–55, 2006.

Hoffman, M. J., Catania, G. A., Neumann, T. A., Andrews, L. C., and Rumrill, J. A.: Links between acceleration, melting, and supraglacial lake drainage of the western Greenland Ice Sheet, J. Geophys. Res., 116, F04035, doi:10.1029/2010JF001934, 2011.

Hutter, K.: Theoretical glaciology: material science of ice and the mechanics of glaciers and ice sheets, Dordrecht, 510 pp., 1983.

Jacob, T., Wahr, J., Pfeffer, W. T., and Swenson, S.: Recent contributions of glaciers and ice caps to sea level rise, Nature, 482, 514–518, doi:10.1038/nature10847, 2012.

Kargel, J. S., Ahlstrøm, A. P., Alley, R. B., Bamber, J. L., Benham, T. J., Box, J. E., Chen, C., Christoffersen, P., Citterio, M., Cogley, J. G., Jiskoot, H., Leonard, G. J., Morin, P., Scambos, T., Sheldon, T., and Willis, I.: Brief Communication: Greenland's shrinking ice cover: "fast times" but not that fast, The Cryosphere Discuss., 5, 3207–3219, doi:10.5194/tcd-5-3207-2011, 2011.

Kaser, G., Cogley, J. C., Dyurgerov, M. B., Meier, M. F., and Ohmura, A.: Mass balance of glaciers and ice caps: Consensus estimates for 1961–2004, Geophys. Res. Lett., 33, 1–5, 2006.

Knudsen, N. T. and Hasholt, B.: Radio-echo Sounding at the Mittivakkat Gletscher, Southeast Greenland, Arct. Antarct. Alp. Res., 31, 321–328, 1999.

Knudsen, N. T. and Hasholt, B.: Mass balance observations at Mittivakkat Glacier, southeast Greenland 1995–2002, Nord. Hydrol., 35, 381–390, 2004.

Knudsen, N. T., Nørnberg, P., Yde, J. C., Hasholt, B., and Heinemeier, J.: Recent marginal changes of the Mittivakkat Glacier, Southeast Greenland and the discovery of remains of reindeer (*Rangifer tarandus*), polar bear (*Ursus maritimus*) and peaty material, Danish J. Geogr., 108, 137–142, 2008.

Liston, G. E. and Mernild, S. H.: Greenland freshwater runoff. Part I: A runoff routing model for glaciated and non-glaciated landscapes (HydroFlow), J. Climate, accepted, 2012.

Liston, G. E. and Sturm, M.: A snow-transport model for complex terrain, J. Glaciol., 44, 498–516, 1998.

Meier, M. F., Dyurgerov, M. B., Rick, U. K., O'Neel, S., Pfeffer, W. T., Anderson, R. S., Anderson, S. P., and Glazovsky, A. F.: Glaciers dominate eustatic sea-level rise in the 21st century, Science, 317, 1064–1067, 2007.

Mernild, S. H. and Hasholt, B.: Climatic control on river discharge simulations, Mittivakkat Glacier catchment, Ammassalik Island, SE Greenland, Nord. Hydrol., 37, 327–346, 2006.

Mernild, S. H. and Liston, G. E.: Greenland freshwater runoff. Part II: Distribution and trends, 1960–2010. Spatial runoff distribution and trends from Greenland to adjacent seas, 1960–2010, J. Climate, accepted, 2012.

Mernild, S. H., Hansen, B. U., Jakobsen, B. H., and Hasholt, B.: Climatic conditions at the Mittivakkat Glacier catchment (1994–2006), Ammassalik Island, SE Greenland, and in a 109 years term perspective (1898–2006), Danish J. Geogr., 108, 51–72, 2008.

Mernild, S. H., Liston, G. E., Steffen, K., van den Broeke, M., and Hasholt, B.: Runoff and mass-balance simulations from the Greenland Ice Sheet at Kangerlussuaq (Søndre Strømfjord) in

a 30-year perspective, 1979–2008, The Cryosphere, 4, 231–242, doi:10.5194/tc-4-231-2010, 2010.
Mernild, S. H., Knudsen, N. T., Lipscomb, W. H., Yde, J. C., Malmros, J. K., Hasholt, B., and Jakobsen, B. H.: Increasing mass loss from Greenland's Mittivakkat Gletscher, The Cryosphere, 5, 341–348, doi:10.5194/tc-5-341-2011, 2011a.
Mernild, S. H., Knudsen, N. T., and Hanna, E.: Mittivakkat Gletscher, SE Greenland, in: The Arctic Report Card, Greenland, edited by: Richter-Menge, J., Jeffries, M. O., Overland, J. E., NOAA Report 2011, available at: http://www.arctic.noaa.gov/report11/greenland_ice_sheet.html, 2011b.
Mernild, S. H., Malmros, J. K., Knudsen, N. T., and Yde, J. C.: Multi-decadal marine and land-terminating glacier recession in the Ammassalik region, Southeast Greenland, The Cryosphere Discuss., 6, 531–561, doi:10.5194/tcd-6-531-2012, 2012a.
Mernild, S. H., Seidenkrantz, M.-S., Chylek, P., Liston, G. E., and Hasholt, B.: Climate-driven fluctuations in freshwater to Sermilik Fjord, East Greenland, during the last 4000 years, Holocene, 22, 155–164, doi:10.1177/0959683611431215, 2012b.
Müller, F. and Iken, A.: Velocity Auctuations and water regime of Arctic valley glaciers. Union Géodésique et Géophysique Internationale. Association Internationale d'Hydrologie Scientifique. Commission de Neiges et Glaces. Symposium on the Hydrology of Glaciers, Cambridge, 7–13 September 1969, 165–182, 1973.
Oerlemans, J., Dyurgerov, M., and van de Wal, R. S. W.: Reconstructing the glacier contribution to sea-level rise back to 1850, The Cryosphere, 1, 59–65, doi:10.5194/tc-1-59-2007, 2007.
Østrem, G. and Brugman, M.: Glacier mass balance measurements. A manual for field and office work, NRHI Science Report, No. 4, 224 pp., 1991.
Parizek, B. R. and Alley, R. B.: Implications of increased Greenland surface melt under global-warming scenarios: Ice-sheet simulations, Quaternary Sci. Rev., 23, 1013–1027, 2004.
Payne, A. J. and Dongelmans, P. W.: Self-organization in the thermomechanical flow of ice sheets, J. Geophys. Res., 102, 12219–12233, 1997.
Pimentel, S. and Flowers, G. E.: A numerical study of hydrologically driven glacier dynamics and subglacial flooding, P. R. Soc. A., 467, 537–558, doi:10.1098/rspa.2010.0211, 2011.
Radić, V. and Hock, R.: Regional and global volumes of glaciers derived from statistical upscaling of glacier inventory data, J. Geophys. Res., 115, F01010, doi:10.1029/2009JF001373, 2010.

Schoof, C.: Ice sheet acceleration driven by melt supply variability, Nature, 468, 803–806, doi:10.1038/nature09618, 2010.

Shepherd, A., Hubbard, A., Nienow, P., King, M., McMillan, M., and Joughin, I.: Greenland ice sheet motion coupled with daily melting in late summer, Geophys. Res. Lett., 36, L01501, doi:10.1029/2008GL035758, 2009.

Sole, A. J., Mair, D. W. F., Nienow, P. W., Bartholomew, I. D., King, M. A., Burke, M. J., and Joughin, I.: Seasonal speedup of a Greenland marine-terminating outlet glacier forced by surface melt-induced changes in subglacial hydrology, J. Geophys. Res., 116, F03014, doi:10.1029/2010JF001948, 2011.

Sundal, A. V., Shepherd, A., Nienow, P. W., Hanna, E., Palmer, S., and Huybrechts, P.: Melt-induced speed-up of Greenland ice sheet offset by efficient subglacial drainage, Nature, 469, 521–524, doi:10.1038/nature09740, 2011.

Tachikawa, T., Kaku, M., Iwasaki, A., Gesch, D., Oimoen, M., Zhang, Z., Danielson, J., Krieger, T., Curtis, B., Haase, J., Abrams, M., Crippen, R., and Carabajal, C.: ASTER Global Digital Elevation Model Version 2 – Summary of Validation Results, NASA Land Processes Distributed Active Archive Center and the Joint Japan-US ASTER Science Team, available at: https://igskmncnwb001.cr.usgs.gov/aster/GDEM/Summary_GDEM2_validation_report_final.pdf, 2011.

Truffer, M., Harrison, W. D., and March, R. S.: Correspondance, J. Glaciol., 51, 663–664, 2005.

van der Wal, R. S. W., Boot, W., van den Broeke, M., Smeets, C. J. P. P., Reijmer, C. H., Donker, J. J. A., and Oerlemans, J.: large and rapid Melt-Induced Velocity Changes in the Ablation Zone of the Greenland Ice Sheet, Science, 321, 111–113, 2008.

Vincent, C., Soruco, A., Six, D., and Le Meur, E.: Glacier thickening and decay analysis from 50 years of glaciological observations performed on Glacier d'Argentière, Mont Blanc area, France, Ann. Glaciol., 50, 73–79, 2009.

Yde, J. C. and Knudsen, N. T.: 20th-century glacier fluctuation on Disko Island (Qeqertarsuaq), Greenland, Ann. Glaciol., 46, 209–214, 2007.

Zwally, H., Abdalati, W., Herring, T., Larsen, K., Saba, J., and Steffen, K.: Surface melt-induced acceleration of Greenland ice-sheet flow, Science, 297, 218–222, doi:10.1126/science.1072708, 2002.

Table 1. Calculated and observed ice surface velocity for stake 60 in the center of the ablation zone for the beginning (1996) and the end (2011) of the observation period. v_{sia} is calculated from Eq. (5), and v_{obs} is observed velocity.

	Ice thickness (m)	Surface slope ($m\,m^{-1}$)	v_{sia}	v_{obs}
1996	140	0.084	16.6	18.8
2011	104	0.079	4.2	8.2

TCD
6, 2005–2036, 2012

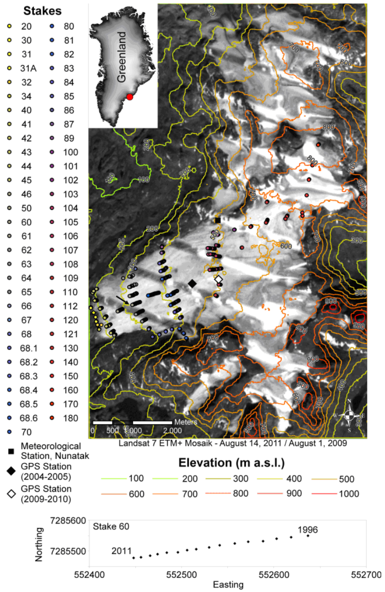

Fig. 1a. The Mittivakkat Gletscher (26.2 km^2, where the measured mass-balance area is 17.6 km^2; 65°41 N, 37°48 W) including topographic map (100-m contour interval), and circles illustrating the stake locations for the glacier observation program, 1995 through 2011. The stake colors on the glacier surface correspond to the stake numbers illustrated to the left. Due to a high density of crevasses in the SE part of the glacier, no stakes were located there. The meteorological station at the nunatak is shown by a black square and the GPS station on the glacier by black and white diamonds. The inset figure indicates the location of the Mittivakkat Gletscher in Southeastern Greenland. Below, an example of an annual time series (1996–2011) of stake locations is shown for stake 60, denoted by a black arrow on the map (source: Landsat 7 ETM+ Mosaic, 14 August, 1 August 2011, 2009).

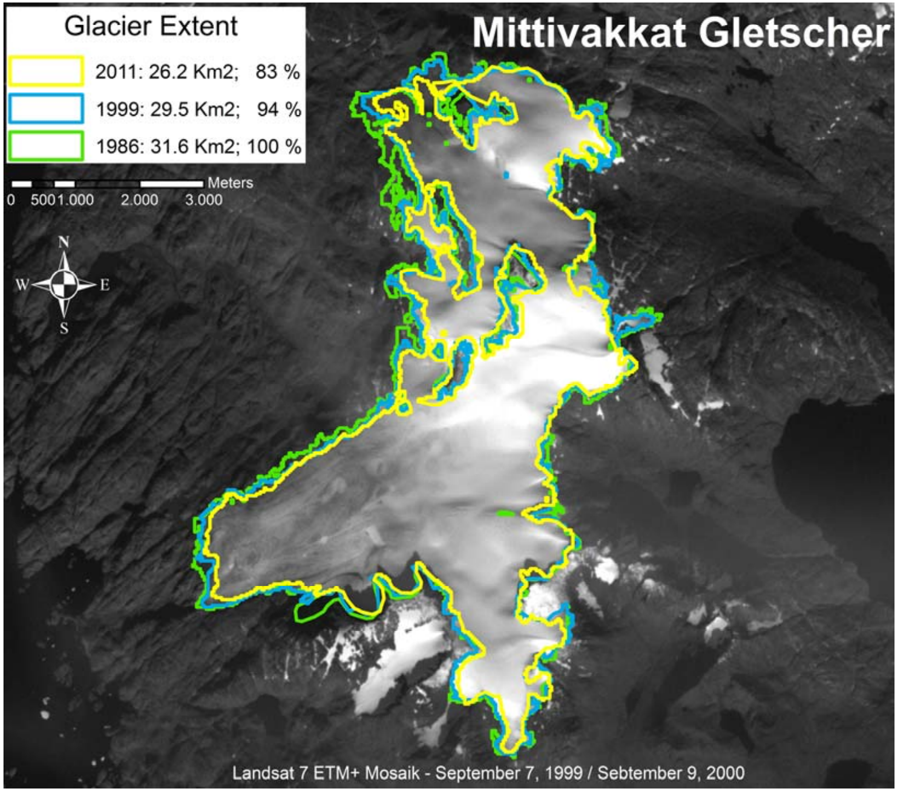

Fig. 1b. Margin position and area for the Mittivakkat Gletscher in 1986, 1999, and 2011, based on Landsat 5 TM observations (11 September 1986) and Landsat 7 ETM+ Mosaic (7 September 1999, and 14 August 2011) (source – background image: Landsat 7 ETM+ Mosaic 1999/00) (updated from Mernild et al., 2011a).

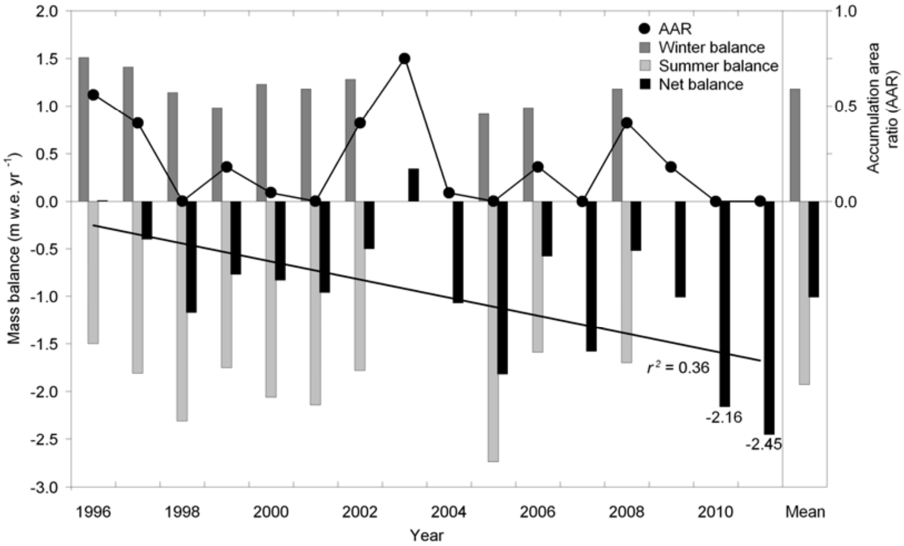

Fig. 2. Observed winter, summer, and net annual mass balance and accumulation area ratio for Mittivakkat Gletscher, 1995/96 to 2010/11. Note that winter and summer balances have not been observed for each individual year. The data sets reported here are updated from Mernild et al. (2011a).

TCD
6, 2005–2036, 2012

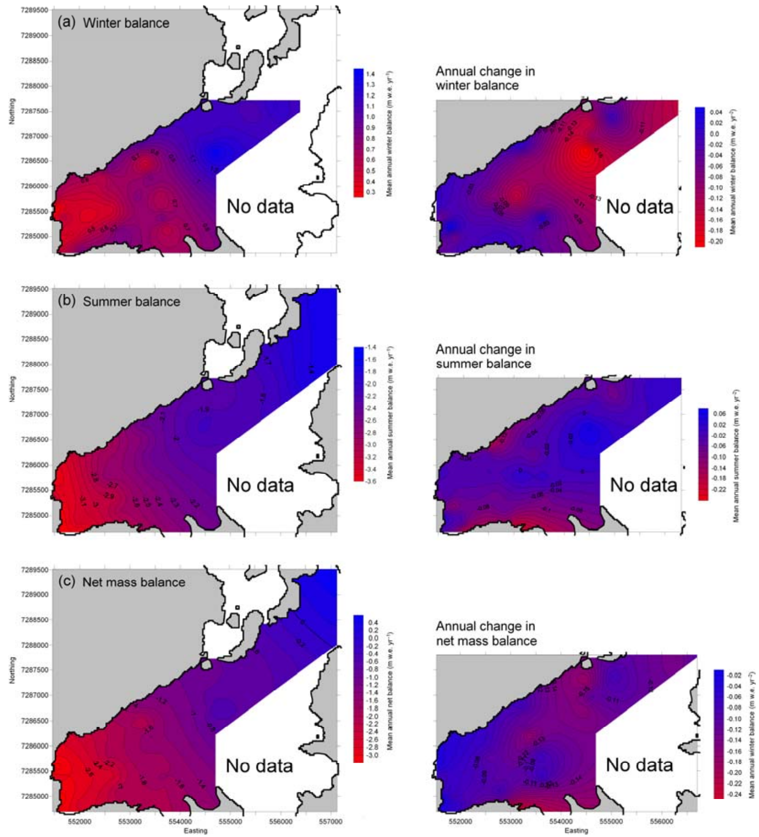

Fig. 3. Annual mass balance distributions and changes at Mittivakkat Gletscher: **(a)** mean winter mass balance and annual change (blue-red shades); **(b)** mean summer mass balance and annual change; and **(c)** net annual mass balance and annual change for 1996/97 through 2010/11. The white area has no data, and the margin is estimated based on Landsat 7 ETM+ Mosaic – 14 August 2011 and 1 August 2009.

TCD
6, 2005–2036, 2012

Recession of Greenland's Mittivakkat Gletscher

S. H. Mernild et al.

Title Page
Abstract | Introduction
Conclusions | References
Tables | Figures
◀| |▶
◀ ▶
Back | Close
Full Screen / Esc
Printer-friendly Version
Interactive Discussion

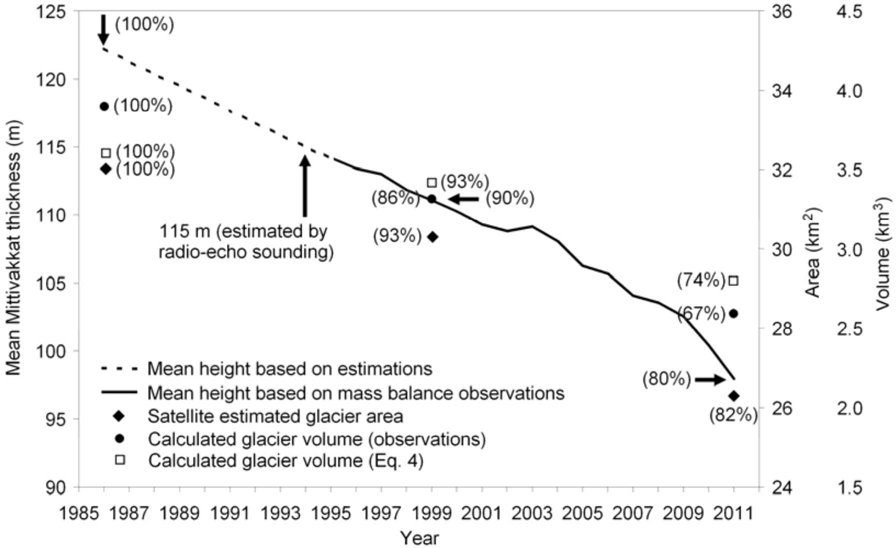

Fig. 4. Time series of estimated mean thickness (line), area (diamonds), and volume (circles) for the Mittivakkat Gletscher. In 1994 the mean thickness was estimated by radio-echo sounding (Knudsen and Hasholt 1999). The dashed time series is estimated based on a linear extrapolation of the observed 1995/96 to 2010/11 mean trend. The percent change since 1986 (the 1986 values were set to 100 %) is shown in brackets.

TCD
6, 2005–2036, 2012

Recession of Greenland's Mittivakkat Gletscher

S. H. Mernild et al.

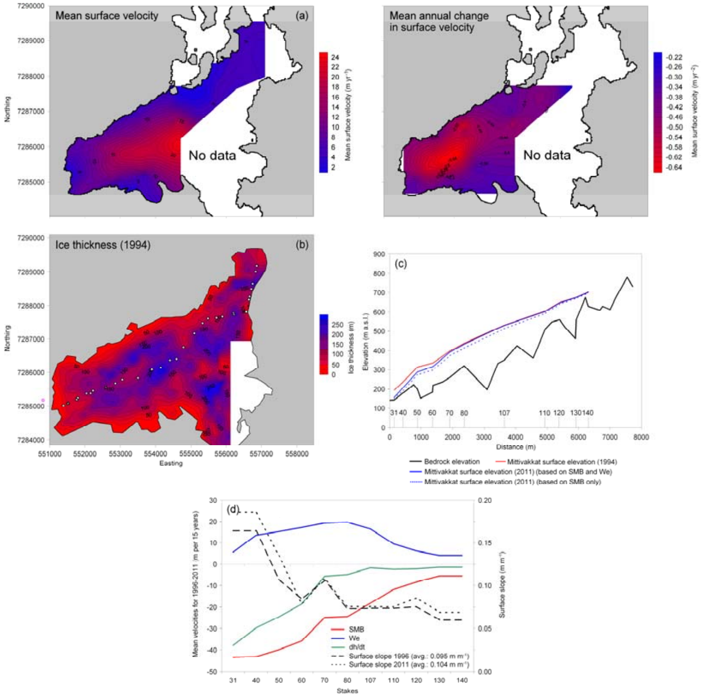

Fig. 5. Mittivakkat Gletscher **(a)** mean annual surface velocity and changes from 1996/97 to 2010/11 (blue-red shades); **(b)** ice thickness based on radar observations in 1994 (Knudsen and Hasholt, 1999) including the location of the longitudinal profile; **(c)** longitudinal mean surface elevation and elevation changes from 1994 to 2011 based on calculations with and without vertical velocity (w_e), showing the positions of stakes 31 to 140; and **(d)** longitudinal mean surface slope for 1996 and 2011, SMB, W_e, and dh/dt. No observations were made in the south-eastern part of the glacier since this is a heavy crevassed area. At two cirques to the south, the spatial mean velocity field might not be representative due to limited observations. The glacier margin in figure **(a)** is estimated from Landsat 7 ETM+ Mosaic – 14 August 2011 and 1 August 2009, and in figure **(b)** from GPS observations.

TCD
6, 2005–2036, 2012

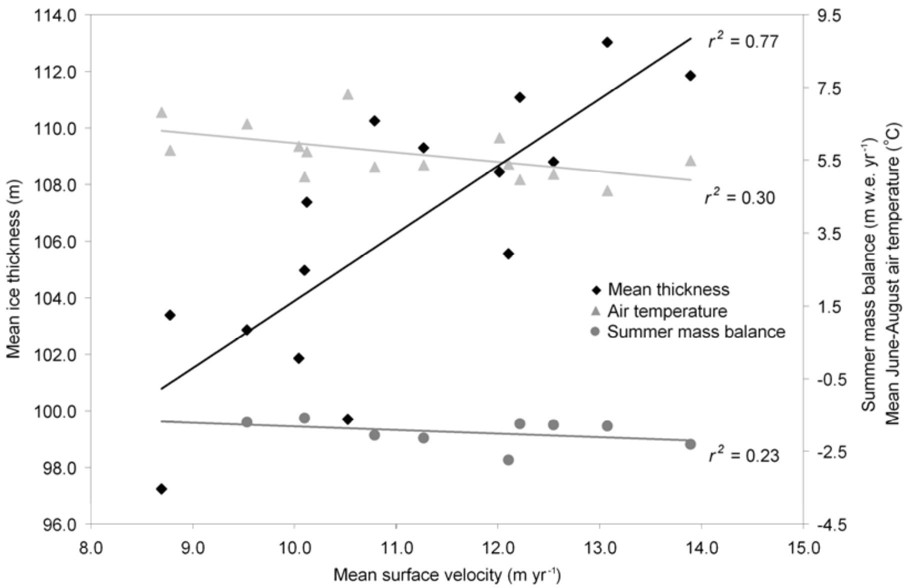

Fig. 6. Linear relation between Mittivakkat Gletscher mean annual surface velocity and mean ice thickness (black diamonds) estimated from stake observations; observed summer mass balance (dark gray circles); and observed mean JJA air temperature at Station Nunatak (light gray triangles) from 1996–2011.

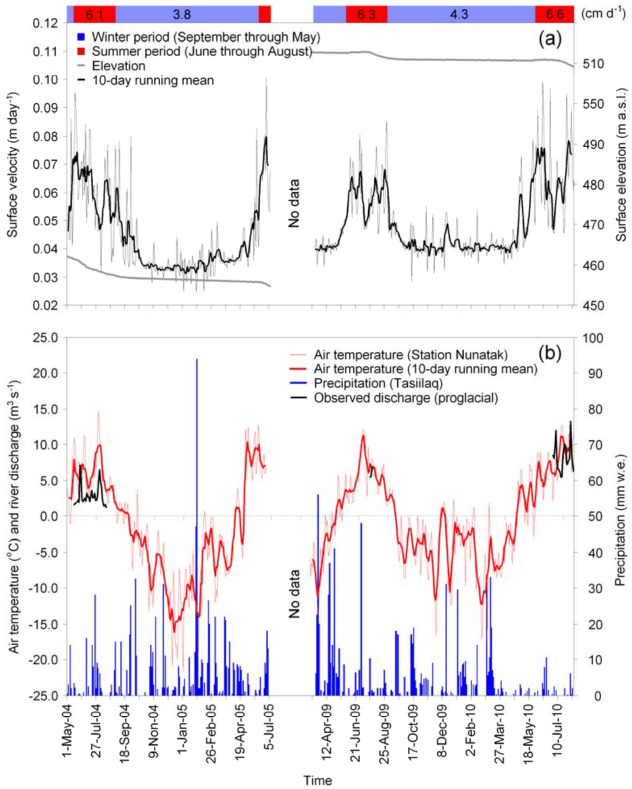

Fig. 7. (a) Observed Mittivakkat Gletscher seasonal surface velocity at the GPS station. Between 2005 and 2009 the GPS station was moved to a higher elevated location on the glacier (see black and white diamonds on Fig. 1 for locations). Also, the mean seasonal surface velocities are shown for the winter (September through May; marked with light blue at the top of the figure) and summer (June through August, marked with red); **(b)** observed air temperature at Station Nunatak, observed precipitation (uncorrected) at Station Tasiilaq, and observed proglacial river discharge drainage 1.5 km downstream from the glacier margin.

TCD

6, 2005–2036, 2012

Recession of Greenland's Mittivakkat Gletscher

S. H. Mernild et al.

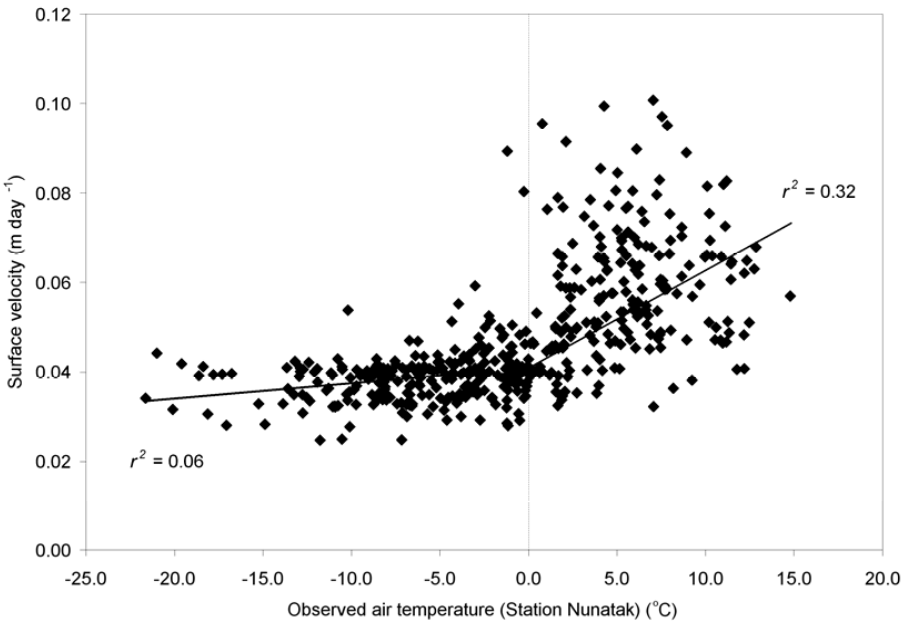

Fig. 8. Relationship between daily Mittivakkat Gletscher surface velocity (observed at the GPS station) and observed air temperature at Station Nunatak from May 2004 through July 2005 and March 2009 through August 2010.